1982-08-15

Diffusion Thermoeffect Measurements of Heats of Transport in Ternary Liquid Toluene Chlorobenzene Bromobenzene Mixtures at 25°C and 3°C

Richard L. Rowley
rowley@byu.edu

Gerald Platt

See next page for additional authors

Original Publication Citation
G. Platt, G. Fowler, T. Vongvanich, and R.L. Rowley, "Diffusion Thermoeffect Measurements of Heats of Transport in Ternary Liquid Toluene Chlorobenzene Bromobenzene Mixtures at 25 degrees C and 35 degrees C", J. Chem. Phys. 77, 2121 (1982)

Diffusion thermoeffect measurements of heats of transport in ternary liquid toluene–chlorobenzene–bromobenzene mixtures at 25° and 35 °C

G. Platt,[a] T. Vongvanich, G. Fowler,[b] and R. L. Rowley

Department of Chemical Engineering, Rice University, Houston, Texas 77251
(Received 8 April 1982; accepted 6 May 1982)

Heats of transport in ternary nonelectrolyte liquid mixtures have been directly measured for the first time. Diffusion thermoeffect measurements have been made for ternary mixtures of toluene–chlorobenzene–bromobenzene at 25 ° and 35 °C. A new boundary sharpening technique was used in addition to a liquid gate withdrawal method. Both techniques yield consistent, accurate values of the heat of transport, but the new cell provides versatility in allowable densities and compositions of the initial phases. Heats of transport were obtained by nonlinear least-squares fitting of calculated to experimental temperature differences measured at positions symmetric about the initial diffusional interface. The two independent heats of transport, obtained by performing two runs with different starting composition gradients for each mean composition, were each fit to a polynomial in temperature and composition. The resultant analytical expression is valid only in the region bounded by $0.1 \leq w_i \leq 0.6 (i = 1,2)$ and $w_3 \geq 0.1$, where the composition is far enough from the binary limits that both of the two heats of transport remain defined and independently determinable. The results obtained for the heats of transport show a direct dependence on temperature and a strong dependence on the relative amount of the heavy component, bromobenzene. These facts are consistent with a proposed interpretive model of the diffusion thermoeffect.

I. INTRODUCTION

Not only will a temperature gradient give rise to a heat flux in multicomponent mixtures, but so also will composition gradients (more appropriately, isothermal chemical potential gradients). This latter effect, known as the diffusion thermoeffect or the Dufour effect, is characterized by a transport property called the heat of transport. The heat of transport of component i, Q_i^* relates the magnitude of the produced heat flux to the diffusional flux of component i under isothermal conditions. Just as there are only $n-1$ independent diffusional fluxes in an n component system, there are also only $n-1$ independent heats of transport. These transport coefficients are of interest because they contain significant information concerning the actual energy-diffusional relationship of molecular interactions.[1,2] Study of heats of transport should aid in the development of a generalized theory of transport processes.

In the companion paper to this one,[3] hereafter referred to as PVR1, the phenomenology of the diffusion thermoeffect was described. Moreover, the composition and energy partial differential equations describing the diffusion thermoeffect in ternary systems were solved subject to initial and boundary conditions designed to maximize and facilitate experimental measurement of the two independent heats of transport. Further modeling was done in that paper to provide information relative to thermocouple positioning, parameter optimization, parameter decoupling, expected temperature responses for different conditions and thermophysical properties, and elimination of heat of mixing problems. This work is based on the foundation provided in PVR1; it uses the equations and experimental suggestions of PVR1 to determine Q_1^* and Q_2^* as a function of composition and temperature in ternary mixtures of toluene–chlorobenzene–bromobenzene.

Heats of transport in gas mixtures have been measured by several investigators[4–8]; quantitative measurements in liquid mixtures were thought to be quite impossible.[9] The work of Ingle and Horne[10] and of Rowley and Horne,[11,12] however, established the diffusion thermoeffect as an accurate and reliable method of obtaining liquid heats of transport in binary systems. The work reported in PVR1 indicates that successful multicomponent diffusion thermoeffect experiments can be carried out in an adiabatic boundary cell with an initially sharp, isothermal compositional gradient as the driving force if (1) temperature differences of points symmetric about the initial interface are measured as a function of time and (2) two experiments with different initial starting gradients are performed at each mean or bulk composition in order to decouple the heats of transport.

The solution of the composition and energy equations in PVR1 was obtained using a double perturbation technique. The thermophysical properties were expanded in a Taylor's series expansion about the mean composition while the cross diffusion terms in the composition equation were treated as a perturbation to the straight diffusion terms. It was shown that the zeroth order composition solution was sufficient for those systems which have small cross diffusion coefficients relative to the straight coefficients. Furthermore, the zeroth order solution to the temperature equation is by far the predominant term in the expansion unless the system shows a large compositional dependence in its thermophysical properties. For composition independent properties, the zeroth order solution is in fact the exact solution.

The toluene–chlorobenzene–bromobenzene system was chosen for this work because of the availability

[a]Present address: E.D.H., Texaco, Inc., Houston, Texas 77052.

[b]Present address: Baylor College of Medicine, Houston, Texas 77025.

 0021-9606/82/162121-09$02.10

of diffusion coefficient data and the moderate composition dependence of its thermophysical properties. For this system, the zeroth order temperature solution is adequate and should provide values for the heat of transport within the combined precision limits of the thermophysical properties, the experimental technique, and the parameter estimation procedure; we estimate this to be roughly 10%. Temperature differences were measured between points symmetric about the interface to eliminate the heat of mixing effect as discussed in PVR1. Under these conditions, Eq. (3.16) of PVR1 applies:

$$\Delta T(z') = (4/a^2\bar{C}_p)\sum_{i=1}^{2}(Q_1^* D_{1i} + Q_2^* D_{2i})[(\Delta w_i)/(\theta_{ii}^{-1} - \tau^{-1})] \times \sum_{l=1}^{\infty}(-1)^l F_{il}\sin[(2l-1)\pi z'/a], \quad (1.1)$$

where

$$F_{il} = \pi(-1)^l\{\exp[-(2l-1)^2 t/\theta_{ii}] - \exp[-(2l-1)^2 t/\tau]\}/(2l-1), \quad (1.2)$$

$$\tau = \rho\bar{C}_p a^2/\pi^2 k, \quad (1.3)$$

$$\theta_{ii} = a^2/\pi^2 D_{ii}, \quad (1.4)$$

z' is distance of either thermocouple probe from the initial interface (both thermocouples are equidistant from the interface), a is total cell height, $\bar{C}_p$ is specific heat, D_{ij} are mutual diffusion coefficients, Δw_i is the initial composition of component i in the upper phase minus that of the lower phase, ρ is density, and k is thermal conductivity.

Equations (1.1)–(1.4) form the basis for obtaining Q_1^* and Q_2^* from temperature measurements as a function of time. The values for a particular composition can be obtained by nonlinear least-squares fitting of calculated and measured temperature differences by treating Q_1^* and Q_2^* as two simultaneously adjustable parameters. However, as was pointed out in PVR1, two experiments must be done at each mean composition in order to decouple the parameters. While there is actually a composition nonuniformity in the system throughout the duration of the experiment, the composition at which the heats of transport are measured is rigorously defined by the Taylor's series expansion performed in obtaining the final solution. Thus, all properties are to be evaluated at the mean or average mass fraction located at the center of the cell about which the expansion was made. Hence, values of thermophysical properties, including the obtained heats of transport, are evaluated at $w_{iA} = (w_{iU} + w_{iL})/2$ for each component, where w_{iU} and w_{iL} represent the initial upper and lower phase compositions, respectively, of component i.

II. EXPERIMENTAL

Rowley and Horne[12] developed a liquid-gate withdrawal cell for measurement of heats of transport in binary liquid mixtures. Highly accurate heats of transport can be obtained by this technique as evidenced by the agreement shown between Onsager coefficients obtained from diffusion thermoeffect experiments and those obtained from thermal diffusion factors.[11] The disadvantages of this type cell are that the gate fluid must be immiscible in all other components and must further have a density intermediate to the two initial phases. This becomes a burdensome requirement for ternary systems because two independent experiments must be performed at each mean composition with different initial composition differences. In order to fit both Q_1^* and Q_2^* the composition differences must be large enough to decouple the parameters which often requires mixtures out of the proper density range.

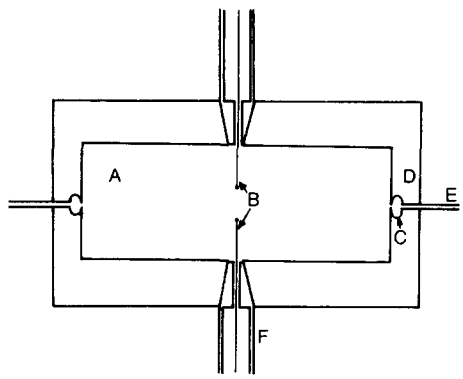

FIG. 1. Schematic diagram of liquid gate withdrawal cell. A. Cell chamber. B. Thermocouples. C. Cell equatorial rim. D. Vacuum jacket. E. Withdrawal ports. F. Ground glass fittings for support of thermocouples and filling and venting of cell.

A new type of cell was designed to provide much more versatillity in initial interface creation. The boundary sharpening cell developed is based on the concept used in Tiselius diffusion cells, sharpening an initially somewhat diffuse interface by siphoning out fluid at the interfacial level.[13] To eliminate any possibility of a cell-dependent systematic error, the two runs required for analysis of Q_1^* and Q_2^* at each mean composition were made in the two different types of boundary formation cells.

The liquid-gate withdrawal cell used in this work was similar to that used by Rowley and Horne. A schematic diagram is shown in Fig. 1. Details of the liquid-gate withdrawal technique and use of this type of cell are given elsewhere.[12] This particular cell measured 3.00 cm in height and 6.0 cm in diameter. The outer jacket was evacuated following thermal equilibration to provide adiabatic boundary conditions. Thermocouple leads were secured, at positions symmetric about the interface, with a "filled epoxy" into small ground glass fittings, which also served as filling ports. Thermocouple beads were made by arc welding precision 40 gage copper and constantan wires. Bead sizes were consistently of radius 0.2 mm. Bead locations were measured visually with a measuring cathetometer; uncertainty in the temperature measurement loci is equivalent to bead radius of ±0.2 mm. A circumferential rim or bulge at cell half-height contained a narrow ring opening into the cell and thereby provided fixation of the interface locus as well as a microreservoir for the remainder of the liquid-gate fluid following contact of the upper and lower phases. This rim has been shown to be required for this type of cell in order to prevent

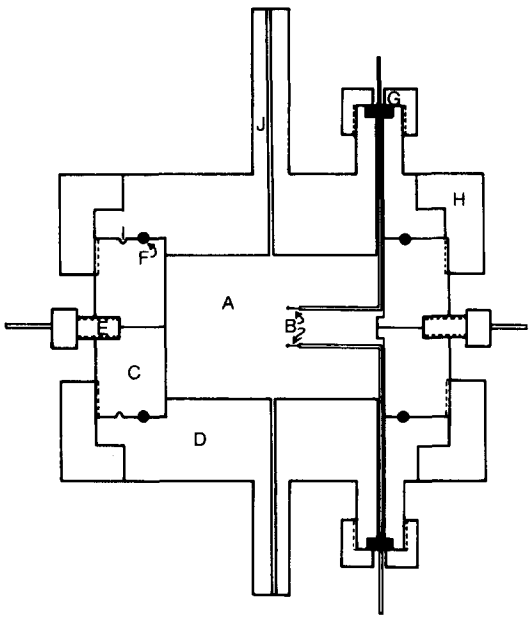

FIG. 2. Schematic diagram of boundary sharpening cell. A. Cell chamber. B. Thermocouples. C. Teflon body. D. Teflon end cap. E. Withdrawal ports. F, O-ring. G. Septum and cap for thermocouple lead seal to the tubes attached to micrometer heads. H. Brass securing ring. I. Alignment pin. J. Filling port.

geometrical constriction of the diffusional area by any remaining gate fluid.[12] Water was used as the liquid gate in all of the experiments performed in this cell due to its insolubility in the other components. The solubilities of bromobenzene, chlorobenzene, and toluene in 100 g water at 20 °C are listed in Perry's Handbook[14] as 0, 0.05, and 0.05 g, respectively. Water was withdrawn from four equatorially placed ports at 0.2 cm^3/min. The cell was vibrationally isolated from the room and air bath by layers of sand and foam pads. This ensured a smooth, full-term contact between the two phases. The upper phase, initially contained in a syringe cothermostated in the air bath with the actual cell, was brought into the upper portion of the cell through a small diameter copper tube heat exchanger as the liquid gate was withdrawn.

The second type of cell employed was the boundary sharpening cell diagrammed in Fig. 2. The cell body was machined from a 10 cm diameter Teflon rod such that the inside cell diameter was 3.0 cm. The end caps were also machined from 3.0 cm thick slices of the Teflon rod such that when both caps were seated against their respective O-rings by brass screw caps, inside cell height was 2.97 cm. In this type of cell, adiabatic boundary conditions were maintained due to the thick, low thermal conductivity end caps. Additionally, both the inside and outside surfaces of the end caps were at essentially the same temperature since the entire apparatus was in a constant temperature environment thermally equivalent to the initial cell temperature. Furthermore, cell temperature responses were small so that conduction through the end caps was negligible. Four equatorial 1/64 in. holes were drilled to provide exact boundary formation at cell half-height.

Thermocouples were again made from 40 gage precision copper-constantan thermocouple wire with 0.2 mm bead radius. Thermocouple positions were more accurately controlled in this type of cell as the beads were enclosed in 25 gage stainless steel tubing which was in turn connected to precision micrometer dials; the cell-tubing seal being made with a silicon septum. This arrangement allowed the thermocouple positions to be fixed quite accurately from run to run. Again the uncertainty in position was due to finite bead size ±0.2 mm. The introduction of thermocouple leads into the boundary sharpening cell provided less interference to the diffusion thermoeffect than the liquid-gate cell counterpart. There the leads run vertically through the fluid at the radial center of the cell. This is also where the response is to be measured in accord with Eq. (1.1) which was derived in PVR1 from the one-dimensional, vertical, equations of change. Therefore, some conduction loss through the leads would cause slightly modified readings. In the boundary sharpening cell configuration, the small stainless steel thermocouple sheath is secured in a snug, narrow and shallow, groove in the cell wall (see Fig. 2) where it is removed from the central portion of the cell where the effect is to be measured. The stainless steel tubing has a sharp 90° bend in it to locate the thermocouple bead at the cell's radial center. Because of the diffusion thermoeffect's one-dimensional nature in this type of cell, the temperature response is independent of the radial coordinate, and little interference due to thermocouple leads should occur. The actual thermocouple lead extends from the RTV® sealed end of the tubing about 3 mm to further minimize any disturbance due to the support tubing.

The principle of the boundary sharpening cell is the same as that of the typical Tiselius diffusion cell. An initial interface formed at a three-way stopcock is lowered as the more dense fluid (which initially filled the entire cell) is withdrawn through the side ports. Siphoning of the fluid continues until the mixed fluid in the diffuse boundary has been removed, sharpening the boundary to a distinct sharp interface. Preliminary experiments were conducted in an analogous glass visual cell. Siphon times in the actual Teflon cell were determined from these studies in conjunction with cell dimensions. Interferometric studies have conclusively shown that this type of initial interface formation is superior to most other techniques especially with respect to turbulence.[15] Actual siphon rates were maintained at a constant 1.23 ml/min with a syringe pump until sufficient time had elapsed for boundary sharpening. As with the liquid gate cell, the less dense fluid entering the cell had been cothermostated with the cell. Initiation of the diffusion thermoeffect occurred when the siphoning action of the syringe withdrawal pump was shut off.

Although the fluid is being siphoned at a rate faster than diffusion in order to obtain an initial sharp boundary, there is no guarantee that the isothermal initial condition upon which Eq. (1.1) was based will be maintained. It is therefore imperative to look at the diffusion thermoeffect response for nonuniform initial tem-

perature profiles. Rowley and Horne[16] have simulated various nonuniform initial starting temperatures and found that in all cases, the temperature difference measured between symmetrically located thermocouples relaxes back to that predicted by solution of the energy equation based on the isothermal initial condition; e. g., Eq. (1. 1). This is due to the competing effects of the two portions of the heat flux

$$q = q_c + q_t \,, \tag{2.1}$$

where q_c is the conduction flux due to thermal conduction down the temperature gradient and q_t is the transported heat flux due to heat of transport down the composition gradient. As long as the initial condition for the composition profile matches that used to obtain Eq. (1. 1) the conductive flux will relax back to the proper balance. If a temperature gradient larger than that which should balance the transported heat flux is initially present, more heat is conducted than would be otherwise, and the local temperature relaxes back to that predicted by the diffusion thermoeffect with isothermal initial conditions. If a temperature difference less than that predicted by Eq. (1. 1) exists at short times due to initial temperature nonuniformities then q_c is smaller than otherwise, and again ΔT comes back to that predicted by Eq. (1. 1). This results in a "steady-state" ΔT with respect to the heat being conducted and transported. The steady state ΔT is not constant, however, as the composition, hence the measured temperature difference, slowly changes in time due to diffusion. Temperature response data from the boundary sharpening cell were only used for times greater than 500 s for which Eq. (1. 1) applies even when some temperature nonuniformities exist at the time of boundary formation. Rowley and Horne[16] have shown that 500 s is sufficient time for thermal relaxation back to the steady state ΔT even for quite large initial temperature nonuniformities.

Both cells were mounted on a vibrationally isolated stand in an air bath maintained at the desired run temperature to ± 0. 01 °C. Temperature differences were measured directly by using the lower thermocouple as the reference junction and the upper thermocouple as the measuring junction. As temperature differences were normally less than 0. 3 °C, the Seebeck effect potential difference was amplified by a factor of 500 through a Leeds–Northrup model 9829 linear amplifier. The amplified signal was then periodically logged with a Hewlett–Packard data logger and continuously monitored with a strip chart recorder. In this manner, potential differences of 0. 03 μV were measurable with a corresponding temperature difference resolution of slightly better than 0. 001 °C.

The exact zero of time in the liquid-gate cell was unknown because no visual observation of phase contact could be made due to the smooth layering process. However, the initial ΔT response was obtained from the strip chart recording. A time lag parameter which depends on z' was fit with each run and was added to the initial response time shifting the time coordinate to zero for initial phase contact. The time lag parameter seldom exceeded 15 s and was usually less than 10 s for the z' values used in these experiments. The zero of time for the boundary sharpening cell is precisely known; it is the time at which the siphon pump is turned off.

All mixtures were prepared gravimetrically from "Baker analyzed" reagent grade pure components without further purification. Distilled, deionized water was used for the liquid-gate cell experiments.

III. RESULTS

Equation (1. 1) was used to obtain Q_1^* and Q_2^* by simultaneous nonlinear least-squares fitting of two independent data sets, one obtained from an experiment performed in the liquid-gate withdrawal cell, the other obtained in the boundary sharpening cell. Both experiments were performed at the same mean mass fraction for each component but with different initial compositions in the two phases. This provides a stringent test on the accuracy of the boundary sharpening cell since the data obtained in two different cells must fit Eq. (1. 1) simultaneously. In our experience, the goodness of the fit is indicative of the quality of the experiments. A representative example of the quality of data fit obtained from this procedure is shown in Fig. 3. In the fitting procedure, all thermophysical properties are evaluated at the mean mass fraction as required by the perturbation solution discussed in PVR1. The composition and temperature dependence of the thermophysical properties for the toluene(1)–chlorobenzene(2)–bromobenzene(3) system as well as the literature source from which they were obtained are shown in Table I. These equations were directly used to obtain property values for the experimental conditions of each run.

Experiments were performed at various ternary compositions at 25 and 35 °C. No values could be obtained close to the binary limits where the fitting technique could not provide values for both Q_1^* and Q_2^*. This is to be expected since there is only one independent heat of transport in binary mixtures. Care was also taken to insure that proper density differences were maintained between the upper and lower phases so that sharp initial interfaces could be formed in one or the other of the two types of cells. However, this limited the composition region over which the experiments could be performed. Experimental results are shown in Table II.

The compositional dependence of Q_1^* and Q_2^* is not immediately obvious from Table II, therefore Q_1^* and Q_2^* were separately fit as a polynomial in mass fractions. The compositional behavior of Q_1^* and Q_2^* at 25 and at 35 °C are displayed in Figs. 4–7 and are analytically given by

$$\begin{aligned} Q_1^* = (\bar{M} w_1 w_3)[&-29.687 + 0.0706T + 0.08715T w_1 \\ &- (98.70 - 0.418T) w_2 + (787.3 - 2.765T) w_1 w_2 \\ &- 21.59 w_1^2 - 0.1071 T w_2^2] J/g \,, \end{aligned} \tag{3.1}$$

$$\begin{aligned} Q_2^* = (\bar{M} w_1 w_2)[&-39.370 + 0.1302T - 0.01679T w_1 \\ &- (120.6 - 0.4199T) w_2 + (993.7 - 3.308T) w_1 w_2 \\ &+ 7.006 w_1^2 - 0.04601 T w_2^2] J/g \,. \end{aligned} \tag{3.2}$$

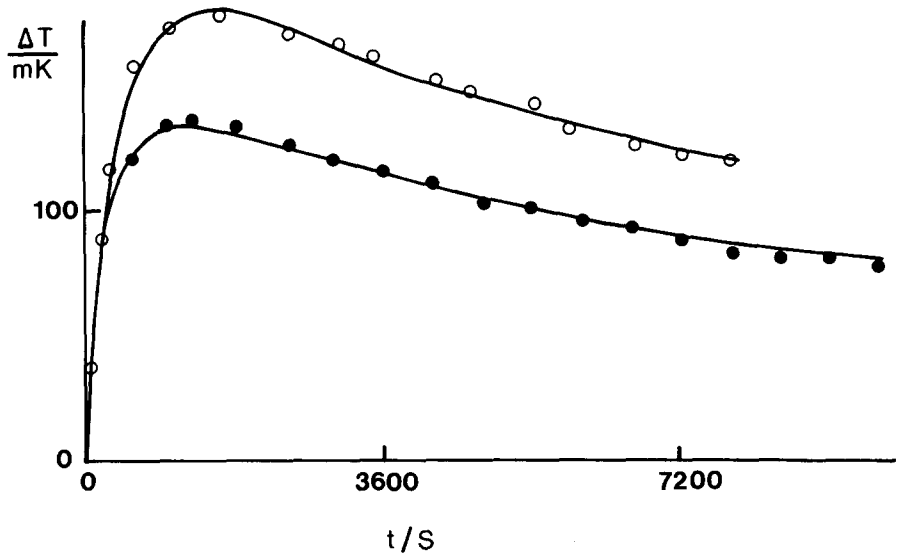

FIG. 3. Simultaneous fit of data at 25°C, $w_{1A}=0.397$, and $w_{2A}=0.303$ taken with liquid gate withdrawal cell, —o—, and with the boundary sharpening cell, —●—. The points represent the measured ΔT in millikelvins while the curves are predicted ΔT based on best fit Q_1^* and Q_2^*. Run conditions in the liquid gate cell were $\Delta w_1=+0.795$, $\Delta w_2=-0.195$ while in the boundary sharpening cell $\Delta w_1=+0.794$, and $\Delta w_2=-0.406$.

The goodness of the fit of the data to empirical Eqs. (3.1) and (3.2) is also shown in Table II.

IV. DISCUSSION

It is evident from the standard deviations shown in Table II that the analysis procedure for diffusion thermoeffect data for this system yields more reliable Q_1^* results than Q_2^*. This appears to be due to the relative magnitudes of Q_1^* and Q_2^*. The simulation of the diffusion thermoeffect done in PVR1 indicated that for this system and under conditions similar to the runs performed in this work, a change in the value of Q_1^* produced a much larger variation in the measured ΔT than an equivalent change in the value of Q_2^*. It was also shown, and is evident from Eq. (1.1), that Q_1^* and Q_2^* affect the magnitude of the ΔT response but not the time dependent shape. Actually it is not Q_1^* that directly affects ΔT, but rather the product $Q_1^* D_{i1} \Delta w_i$. Since the cross diffusion terms are small, the main effect is from $Q_1^* D_{11} \Delta w_1$. In the case of the numerical simulations, the larger sensitivity of ΔT to Q_1^* is due to larger input values of Δw_1. In the case of the actual experiments, the larger uncertainty in fit Q_2^* values is due to the smaller magnitude of Q_2^* relative to Q_1^*. Experimentally, this effect was reduced in several cases by beginning the experiments with larger values of Δw_2. However, the range of Δw_i values were limited by density considerations; phase densities were necessarily limited by consistency with experimental techniques. In future work, consideration should always be given to the probable magnitude of each Q_i^* and attempts should be made to design experiments which optimize the parameter estimation precision for both Q_i^*. The fit smooth curves of Eqs. (3.1) and (3.2) represent the parameters Q_1^* and Q_2^* fairly well on an absolute basis. Percent deviations from these equations are large at times due to the small absolute value of Q_2^* and the resultant lesser sensitivity to the ΔT fitting procedure.

It should be noted that the fit polynomial equations for Q_1^* and Q_2^* were obtained at the compositions displayed in Table II. This represents a triangular region of composition defined by $0.10 \leq w_i \leq 0.60$ for $i=1$, 2 and $w_3 \geq 0.1$. Data reduction on experiments performed outside of this region did not lead to independent values for Q_1^* and Q_2^* because in the limit of the three binary systems, only one heat of transport is independent. Thus, Eqs. (3.1) and (3.2) should be used only within the region defined above as is the case with Figs. 4–7. Within this region, interpolative values of Q_1^* and Q_2^* can be expected to be quite accurate; extrapolative estimates from these analytical expression should not be made.

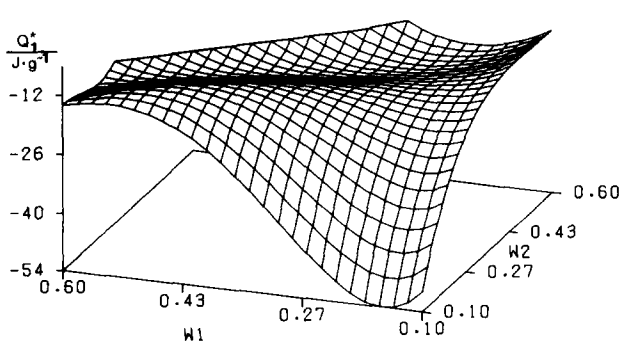

FIG. 4. Compositional dependence of Q_1^* at 25°C from Eq. (3.1).

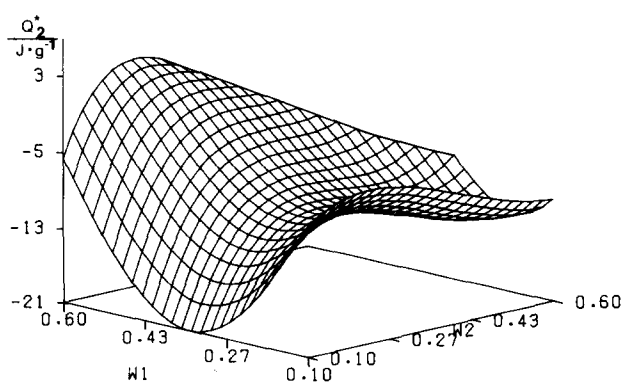

FIG. 5. Compositional dependence of Q_2^* at 25°C from Eq. (3.2).

TABLE I. Thermophysical properties for the toluene (1)–bromobenzene(2)–chlorobenzene(3) system.

Part A-defining equations

(1). Density (kg/m^3) — Ref. 17

$$\rho = \bar{M} \Big/ \left(\sum_{i=1}^{3} x_i V_i^0 + \sum_{j=1}^{3} \sum_{k=j}^{3} V_{jk}^E \right); \quad V_i^0 = \eta_1 \exp(\eta_2 T) + \eta T^2 + \eta_4 T^3]$$

$$V_{jk}^E = x_j x_k \sum_{l=1}^{3} B_{ljk} (x_j - x_k)^{l-1}; \quad B_{ljk} = \beta_1 + \beta_2 T + \beta_3 T^2$$

(2). Diffusion coefficients (m^2/s) — Ref. 18

$$D_{11} = D'_{13}[(1-x_1)D'_{12} + x_1 D'_{23}]/\psi; \quad D_{12} = x_1 D'_{23}(D'_{13} - D'_{12})/\psi$$

$$D_{22} = D'_{23}[(1-x_2)D'_{21} + x_2 D'_{13}]/\psi; \quad D_{21} = x_2 D'_{13}(D'_{23} - D'_{21})/\psi$$

$$\psi = \sum_{i=1}^{3} x_i D'_{jk} \quad (i \neq j \neq k = 1, 2, 3); \quad D'_{ij} = D'_{ji} = \frac{x_i}{x_j + x_i} D^0_{ij} + \frac{x_j}{x_j + x_i} D^0_{ji}$$

$$D^0_{ij} = (\delta_1 \times 10^{-10})(T) \exp(\delta_2 / T)$$

(3) Specific heat ($kJ/kg \cdot K$) — Ref. 19–25

$$\bar{C}_p = \sum_{i=1}^{3} w_i \bar{C}^0_{p,i} + \sum_{j=1}^{3} \sum_{k=j}^{3} x_j x_k F_{jk} / (M_j x_j + M_k x_k) \quad (j \neq k)$$

$$\bar{C}^0_{p,i} = \gamma_1 + \gamma_2 T^2 + \gamma_3 T^3; \quad F_{jk} = \sum_{l=1}^{3} \xi_l (x_j - x_k)^{l-1}$$

(4). Thermal conductivity ($W/m \cdot K$)

$$k = \sum_{i=1}^{3} w_i k_i^0 + \sum_{i=1}^{3} w_i \sum_{j=1}^{3} w_j G_{ji} (k_{ji} - k_i^0) \Big/ \sum_{l=1}^{3} w_l G_{lj}$$

$$k_i^0 = \zeta_1 - \zeta_2 T; \quad G_{jk} = \exp(-0.3 A_1 / RT); k_{jk} = A_2 k_j^0 + A_3 k_k^0$$

Part B-parameter values

Index	Parameter	$l=1$	$l=2$	$l=3$	$l=4$
$i=1, j=1, k=2$	β_l	-4.9011×10^{-3}	2.5064×10^{-5}	-3.40×10^{-8}	
$i=2, j=1, k=2$	β_l	-2.6431×10^{-3}	1.6793×10^{-5}	-2.66×10^{-8}	
$i=3, j=1, k=2$	β_l	-1.6452×10^{-1}	1.0429×10^{-3}	-1.55×10^{-6}	
$i=1, j=1, k=3$	β_l	5.5969×10^{-2}	-3.5858×10^{-4}	5.68×10^{-7}	
$i=2, j=1, k=3$	β_l	-3.3617×10^{-2}	2.1313×10^{-4}	-3.38×10^{-7}	
$i=3, j=1, k=3$	β_l	1.4532×10^{-1}	-9.2044×10^{-4}	1.46×10^{-6}	
$i=1, j=2, k=3$	β_l	1.3487×10^{-3}	-8.1481×10^{-6}	1.24×10^{-8}	
$i=2, j=2, k=3$	β_l	-2.3303×10^{-4}	1.5887×10^{-6}	-2.70×10^{-9}	
$i=3, j=2, k=3$	β_l	1.2961×10^{-3}	-8.2872×10^{-6}	1.32×10^{-8}	
$i=1$	η_l	8.35773×10^{-2}	5.22475×10^{-4}	1.22126×10^{-6}	-6.667×10^{-10}
$i=2$	η_l	7.98155×10^{-2}	6.82333×10^{-4}	4.90×10^{-7}	0
$i=3$	η_l	7.87366×10^{-2}	1.24020×10^{-3}	-1.46378×10^{-6}	2.0×10^{-9}
$i=1, j=2$	δ_l	2.13001	−1083.34880		
$i=1, j=3$	δ_l	1.94759	−1130.16898		
$i=2, j=1$	δ_l	2.37125	−1033.82635		
$i=2, j=3$	δ_l	1.87852	−1130.16898		
$i=3, j=1$	δ_l	2.28082	−1033.82635		
$i=3, j=2$	δ_l	2.08268	−1083.34880		
$i=1$	γ_l	1.486	-3.861×10^{-6}	1.93×10^{-8}	
$i=2$	γ_l	1.111	0	6.985×10^{-9}	
$i=3$	γ_l	0.879	0	3.253×10^{-9}	
$j=1, k=2$	ξ_l	2.84	1.3	−2.2	
$j=1, k=3$	ξ_l	7.91	−6.5	12.1	
$j=2, k=3$	ξ_l	−8.24	−6.7	6.0	
$j=1, k=2$	A_l	76.951 J/mol	0.4219	0.5889	
$j=1, k=3$	A_l	304.6918 J/mol	0.2771	0.7245	
$j=2, k=1$	A_l	−482.7839 J/mol	0.5889	0.4219	
$j=2, k=3$	A_l	341.6425 J/mol	0.3533	0.6413	
$j=3, k=1$	A_l	−572.4020 J/mol	0.7245	0.2771	
$j=3, k=2$	A_l	−238.0783 J/mol	0.6413	0.3533	
$i=1$	ζ_l	0.2153	2.88×10^{-4}		
$i=2$	ζ_l	0.1991	2.51×10^{-4}		
$i=3$	ζ_l	0.1658	1.98×10^{-4}		

TABLE II. Heats of transport of toluene(1)–chlorobenzene(2)-bromobenzene(3) ternary liquid mixtures at 1 atm.

			Units = kJ/kg					
T/K	w_{1A}	w_{2A}	$-Q_1^*$	σ^a	Deviation from Eq. (3.1)	$-Q_2^*$	σ^a	Deviation from Eq. (3.2)
298	0.100	0.500	18.2	0.5	−3.1	9.3	0.1	−0.6
298	0.200	0.200	20.0	0.1	8.6	5.9	0.2	3.6
298	0.200	0.400	16.5	0.2	2.5	10.3	0.1	−0.2
298	0.200	0.600	20.1	0.1	1.3	11.4	0.3	0.3
298	0.362	0.317	15.9	0.2	0.9	6.1	0.7	1.0
298	0.397	0.303	18.1	0.2	−1.7	9.7	0.4	−3.8
298	0.450	0.174	16.8	0.05	−4.3	9.8	0.2	−1.4
298	0.600	0.200	19.3	0.3	−2.6	−4.1	0.6	1.6
308	0.200	0.200	23.0	0.2	−3.1	−0.2	0.3	−2.0
308	0.200	0.400	19.8	0.1	−2.4	9.7	0.1	−1.7
308	0.200	0.600	21.1	0.1	1.3	13.0	0.3	0.3
308	0.325	0.175	16.4	1.2	0.9	9.7	2.4	1.3
308	0.326	0.274	20.9	0.1	1.3	14.3	0.2	3.4
308	0.397	0.303	25.9	0.2	5.3	22.6	0.3	3.4
308	0.400	0.100	21.3	0.1	−8.7	16.6	0.4	−4.8
308	0.450	0.450	33.9	0.4	−3.5	21.2	0.6	−0.8
308	0.600	0.250	29.6	0.6	5.7	22.4	0.8	−0.1

[a]Linear estimate of standard deviation of the fit parameter.

As Fig. 3 indicates, runs performed in both types of cell agree well. This indicates that no systematic errors occurred and that the boundary sharpening cell can be used, exclusively if desired, to obtain accurate heats of transport. This should permit much more extensive diffusion thermoeffect work as experiments can be performed on those systems for which the liquid gate withdrawal cell is not appropriate. Much more versatility is available with respect to density and constituency when the boundary sharpening cell is used for both runs.

The predominant feature of Q_1^* displayed in Figs. 4–7 is the rapid increase in absolute value as the mass fraction of component three is increased. Why this occurs is not known, but it is evidently correlated with the much larger density and/or higher molecular weight of bromobenzene relative to the other components. Toluene and chlorobenzene have densities which are more similar to each other than they are to bromobenzene and so the compositional effects along lines of constant w_3 are not nearly as large as those along either constant w_1 or w_2. The other significant feature of Q_1^* and Q_2^* is that the absolute value of both generally increases with increasing temperature. This is more clearly observed by comparing actual values in Tables II than from comparison of Figs. 4–7.

There is a known sensitivity of cross transport coefficients, such as the heat of transport, to intermolecular potential parameters in gases.[1,2] Thus, obtaining intermolecular potential parameters using some cross transport coefficient data can lead to more appropriate values than the sole use of diffusivities or thermal conductivities. While theories of liquid mixtures are not as advanced as those of the gas phase, heats of transport should, by the very nature of the phenomenon which they characterize, yield significant information concerning intermolecular interactions. The heat of transport represents the heat transported by the isothermal molecular diffusion of a molecule from a region of one intermolecular environment to a new environment and should therefore provide valuable information about those interactions.

While the data obtained to date for heats of transport

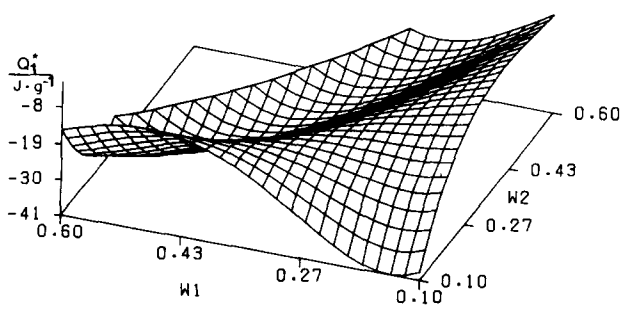

FIG. 6. Compositional dependence of Q_1^* at 35°C from Eq. (3.1).

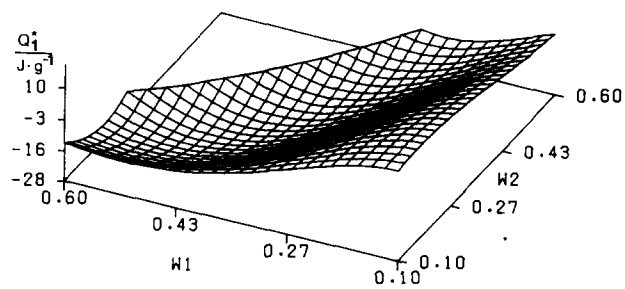

FIG. 7. Compositional dependence of Q_2^* at 35°C from Eq. (3.2).

are insufficient for development of quantitative correlations of theories for the diffusion thermoeffect, we would like to suggest a descriptive model which is consistent with the features of Q_1^* and Q_2^* observed in this study as well as those of Q_1^* measured in binary systems by Rowley and Horne.[12,16] Kinetic interpretations of the heat of transport formulated by Wirtz,[27] Wirtz and Hiby,[28] Denbigh,[29] Prigogine *et al.*,[30] Dougherty and Drickamer,[31] and Rutherford and Drickamer,[32] treat the liquid structure as quasilatticelike. The heat of transport is assumed to be the difference in the local energy of a molecule at one lattice site and its energy at the next site after an energetic jump between the two. This concept, however, is inconsistent with the more fundamental view of diffusion as a randomizing process due to the collisions between molecules in constant thermal motion. Moreover, the diffusion thermoeffect must be related to the actual diffusional process not just the environment in which the molecule finds itself. We propose instead that the heat transported by the diffusional process is inherently coupled to the diffusion mechanism.

In an initially isothermal liquid mixture, the velocities of each molecule vary but obey a distribution law, hence there are molecules which at any one time have velocities larger than the average velocity characteristic of the system temperature. For convenience of discussion, these molecules have an "excess energy" over and above that of their average counterparts. Now when two isothermal phases at different compositions are brought into contact such that mutual diffusion begins, the more energetic molecules will diffuse more rapidly than their average or below average energy counterparts. Although the collisions continuously randomize the energy and velocity of the molecules, the net effect is the diffusion of molecules carrying the excess energy. This same phenomenon occurs in the opposite direction, but the excess energy carried from the two separate original phases is not equivalent because the breadth of the distributions depends on the various properties of the phases. Since the two phases were initially isothermal, the mean energy of the distributions were initially equivalent, but the distribution widths differed because of the constituent component properties. This means that diffusion occurs principally by the more energetic molecules which in turn carry excess energy. The difference between the excess energy carried in the two directions is directly related to the difference in the relative widths of the energy distributions in the two phases and corresponds to the temperature rise and decrease in the two phases as the diffusion thermoeffect occurs.

This picture of the heat of transport is suggested as a model for understanding the trends in the heats of transport as measured in this work. A quantitative theory is not implied. Molecular dynamics simulations of heat effects involved in the diffusional process should be performed to begin development of a theory. Nevertheless, several features of our diffusion thermoeffect are now explicable.

First, the temperature above the interface always warmed due to diffusion while the lower fluid cooled. This is a density effect. The more dense or lower fluid apparently has the widest distribution of energies about the expectation value. Hence, the faster molecules from the more dense phase carry more excess energy than those from the less dense phase. The net result, as the energies of the diffusing molecules are randomized, is an elevation of the average energy of the upper portion of the cell and a lowering of the average energy of the lower portion of the cell. The diffusional process driven by the nonuniformity of chemial potential thereby acts as a natural Maxwell's demon allowing an "energetic" molecule (relative to the lower phase distribution for that component) to move into the top phase and an energetic molecule (relative to the upper phase distribution but "not quite as energetic" relative to the lower phase) to move into the bottom phase.

Secondly, our measurements show a very large density or molecular weight dependence as Q_1^* and Q_2^* change dramatically due to an increased amount of bromobenzene. It must be remembered that Q_1^* is the heat flux per isothermal mass flux of component i under conditions such that all other component mass fluxes except j_n are zero. Thus, two heats of transport are required for ternary systems to describe the transfer of energy due to the two interdiffusional processes between components one and three and between components two and three. The increased bromobenzene concentration has the effect of widening the upper and lower phase energy distributions, due to its larger molecular weight, by differing amounts, thereby increasing the magnitude of Q_1^*.

Thirdly, an increase in temperature would increase the breadth of the energy distributions, but again unequally. One would expect the wider distribution to spread out more than the narrower distribution for a given temperature increase. This corresponds to an increase in the diffusion thermoeffect measured ΔT, consistent with our experiments.

The critical exponent for Q_1^* measured by Rowley and Horne[16] indicates that the heat of transport goes to zero as the liquid–liquid critical temperature is approached along the critical composition line. This is also consistent with the proposed model. As the critical point is approached, the intermolecular correlation length diverges. As the molecules become more correlated, the distribution of energies necessarily narrows. In the limit of perfect correlation, the distributions become spikes at the same mean temperature value. In this idealized limit, all molecules would have the same energy and Q_1^* would be zero.

Although this interpretation of the diffusion thermoeffect views the ΔT response to diffusion as a function of the initial composition differences Δw_i, it does not imply that the Q_1^* are dependent upon the composition gradients. Indeed, they cannot depend upon Δw_i and still be consistent with the assumption of linear force-flux relations. Instead, the Q_1^* must be thought of as the energy differences in the energy distribution widths evaluated in the limit as Δw_i approaches zero.

V. CONCLUSIONS

Heats of transport have been measured in ternary mixtures of toluene–chlorobenzene–bromobenzene as a function of composition at 25 and 35 °C. In so doing, a new type of diffusion thermoeffect cell has been designed and tested which allows a much wider flexibility in mixture measurements than the previously used liquid gate withdrawal cell. The new cell is based on a boundary sharpening technique for the creation of the initial diffusional interface and yields results in excellent agreement with the liquid gate withdrawal cell.

The measured heats of transport show a direct dependence on the temperature and a very strong dependence upon the composition of the mixtures in regions of high bromobenzene concentration. This is presumed due to the much larger density and molecular weight of bromobenzene compared to the relatively close densities of the other two components. These facts are in agreement with a new interpretive model of the diffusion thermoeffect.

As heats of transport are of interest in developing a consistent liquid mixture model and in understanding the liquid mixture structure, more ternary data are required. Additionally, binary heats of transport and their relation to their multicomponent counterparts need to be studied. Compositional and temperature dependencies also require further study. Additionally, several ideal and nonideal systems should be examined to determine the effect chemical consistency and mixture nonidealities have upon the magnitudes of Q_i^*. Finally, it is suggested that molecular dynamics calculations be used to test the appropriateness of the molecular explanation of the diffusion thermoeffect presented here.

ACKNOWLEDGMENT

This material is based upon work supported by the National Science Foundation under Grant No. ENG-7907999.

[1]J. O. Hirschfelder, C. F. Curtiss, and R. B. Bird, *Molecular Theory of Gases and Liquids* (Wiley, New York, 1954).
[2]E. A. Mason, R. J. Munn, and F. J. Smith, Discuss. Faraday Soc. 40, 27 (1965); E. A. Mason, M. Islam, and S. Weissman, Phys. Fluids 7, 1011 (1964).
[3]G. Platt, T. Vongvanich, and R. L. Rowley, J. Chem. Phys. 77, 2113 (1982).
[4]R. P. Rastogi and G. L. Madan, Trans. Faraday Soc. 62, 3325 (1966).
[5]A. Boushehri and S. Afrashtehfar, Bull. Chem. Soc. Jpn. 48, 2372 (1975).
[6]A. Boushehri, J. Chem. Eng. Data 19, 313 (1974).
[7]B. L. Sawford, T. H. Spurling, and D. S. Thurley, Aust. J. Chem. 23, 1311 (1970).
[8]E. A. Mason. L. Miller, and T. H. Spurling, J. Chem. Phys. 47, 1669 (1967).
[9]S. R. deGroot and P. Mazur, *Nonequilibrium Thermodynamics* (North–Holland, Amsterdam, 1962).
[10]S. E. Ingle and F. H. Horne, J. Chem. Phys. 59, 5882 (1973).
[11]R. L. Rowley and F. H. Horne, J. Chem. Phys. 68, 325 (1978).
[12]R. L. Rowley and F. H. Horne, J. Chem. Phys. 72, 131 (1980).
[13]H. J. V. Tyrell, *Diffusion and Heat Flow in Liquids* (Butterworths, London, 1961).
[14]P. E. Liley and W. R. Gambill, *Chemical Engineers' Handbook*, 5th ed., edited by R. H. Perry and C. H. Chilton (McGraw–Hill, New York, 1973).
[15]O. Bryngdahl, Acta Chem. Scand. 12, 684 (1958).
[16]R. L. Rowley and F. H. Horne, J. Chem. Phys. 71, 3841 (1979).
[17]R. K. Nigam and P. P. Singh, Trans. Faraday Soc. 65, 950 (1969).
[18]J. K. Burchard and H. L. Toor, J. Phys. Chem. 66, 2015 (1962).
[19]J. W. Williams and F. Daniels, J. Am. Chem. Soc. 47, 1490 (1925).
[20]R. Tanaka and G. C. Benson, J. Chem. Eng. Data 21, 320 (1976).
[21]R. K. Nigam, P. P. Singh, and N. N. Maini, Indian J. Chem. 8, 908 (1970).
[22]J. Canning and G. H. Cheesman, J. Chem. Soc. 1955, 1230.
[23]S. N. Bhattacharyya, A. V. Anantaraman, and S. R. Palit, Physica (Utrecht) 28, 633 (1962).
[24]B. S. Harsted and E. S. Thomsen, J. Chem. Thermodyn. 7, 369 (1975).
[25]K. Amaya, Bull. Chem. Soc. Jpn. 34, 1349 (1961).
[26]R. L. Rowley, Chem. Eng. Sci. 37, 897 (1982).
[27]K. Wirtz, Ann. Phys. Leipzig 36, 295 (1939).
[28]K. Wirtz and J. W. Hiby, Phys. Z. Leipzig 44, 369 (1943).
[29]K. G. Denbigh, Trans. Faraday Soc. 48, 1 (1952).
[30]I. Prigogine, L. deBrouckere, and R. Armand, Physica (Utrecht) 16, 577 (1950).
[31]E. L. Dougherty and H. G. Drickamer, J. Phys. Chem. 59, 443 (1955); J. Chem. Phys. 23, 295 (1955).
[32]W. M. Rutherford and H. G. Drickamer, J. Chem. Phys. 22, 1157 (1954).